Journal of the American Association for Laboratory Animal Science
Copyright 2024
by the American Association for Laboratory Animal Science

Vol 63, No 4
July 2024
Pages 428–436

Determination of Postmortem Interval in Mice

Rachel R Howie, MS, DVM,[1,*] Michael M McKinney, DVM, DACLAM,[1] Nicholas M Tataryn, DVM, DACLAM,[1] Allysa L Cole, DVM,[2] William D Dupont, PhD,[3] Tzushan S Yang, DVM, PhD, DACVP,[1] and Katherine N Gibson-Corley, DVM, PhD, DACVP[1,*]

Despite the major use of mice in biomedical research, little information is available with regard to identifying their postmortem changes and using that information to determine the postmortem interval (PMI), defined as the time after death. Both PMI and environmental conditions influence decomposition (autolysis and putrefaction) and other postmortem changes. Severe decomposition compromises lesion interpretation and disease detection and wastes limited pathology resources. The goal of this study was to assess postmortem changes in mice in room temperature cage conditions and under refrigeration at 4 °C to develop gross criteria for the potential value of further gross and histologic evaluation. We used 108 experimentally naïve C57BL/6 mice that were humanely euthanized and then allocated them into 2 experimental groups for evaluation of postmortem change: room temperature (20 to 22 °C) or refrigeration (4 °C). PMI assessments, including gross changes and histologic scoring, were performed at hours 0, 4, 8, and 12 and on days 1 to 14. Factors such as temperature, humidity, ammonia in the cage, and weight change were also documented. Our data indicates that carcasses held at room temperature decomposed faster than refrigerated carcasses. For most tissues, decomposition was evident by 12 h at room temperature as compared with 5 d under refrigeration. At room temperature, gross changes were present by day 2 as compared with day 7 under refrigeration. Mice at room temperature lost 0.78% of their baseline body weight per day as compared with 0.06% for refrigerated mice (95% CI for difference 0.67% to 0.76%, $P < 0.0005$). This study supports the consideration of temperature and PMI as important factors affecting the suitability of postmortem tissues for gross and histologic evaluation and indicates that storage of carcasses under refrigeration will significantly slow autolysis.

Abbreviations and Acronyms: IVC, individually ventilated cages; PMI, postmortem interval; RT, room temperature

DOI: 10.30802/AALAS-JAALAS-23-000107

Introduction

Examination of postmortem tissues can be an important diagnostic and research tool. At the time of necropsy, various tissues can be assessed for gross pathologic changes, and samples can be obtained for histopathologic analysis. Histopathology can reveal morphologic tissue changes that correlate with disease processes.[10] Due to the continuum of postmortem changes, the quality of a carcass, and thus its diagnostic utility, are time sensitive and are influenced by numerous environmental factors.[5,11] In most research species, many such factors affect postmortem changes even in a controlled environment. Factors such as room temperature (RT), humidity, or air exchange rates are all tightly regulated in animal housing facilities.[28] No species exemplifies this more than mice, which are commonly housed in individually ventilated cages (IVCs). Mice are often found dead in these cages due to spontaneous natural illness or adverse consequences of research. Although practices vary by institution, mice that are found dead at our institution are immediately placed in a designated carcass refrigerator until the time of necropsy or disposal. Because these carcasses may be exposed to the cage environment or refrigeration for prolonged periods, an important consideration is the differential effect of temperature on postmortem interval (PMI), defined as the time interval since death occurred.[5] We performed a structured assessment of tissue integrity in mice that are found dead at RT in IVC as compared with carcasses that are placed in a standard refrigerator immediately after death to aid in the estimation of PMI. To date, the gross and histologic changes that occur after death have not been accurately described with regard to PMI in mice.[5]

Similarly, no published studies have compared postmortem changes in carcasses maintained under refrigeration or at RT.[9] Descriptions of postmortem changes should be determined under conditions that reflect real-life situations.[9] Mice are often found dead without a known time of death and are then refrigerated pending disposal or future postmortem evaluation. The duration of time spent under refrigeration or at RT can vary, with the maximum conceivable PMI coinciding with an entire cage change interval followed by an indefinite period of refrigeration. Because postmortem sample collection is often delayed for various reasons, diagnosticians should be able to estimate PMI and determine the diagnostic or research value of carcasses under different conditions.

PMI and the associated postmortem changes are permanent, irreversible, and progressive.[5] The degree and type of changes vary with diversity of species and the environment in which they are found can permit subjective judgment on when death occurred.[10] Gross changes such as algor mortis (cooling of the body after death), livor mortis (gravity-dependent pooling of blood identified by red/purple discoloration of the liver, differentiated from blood vessel rupture from a contusion or bruise), rigor mortis (muscle rigidity), tissue desiccation (dehydration of the skin), saponification (hydrolysis of fat), hypostasis (pooling

Submitted: 06 Nov 2023. Revision requested: 14 Nov 2023. Accepted: 27 Feb 2024.
[1]Department of Pathology, Microbiology, and Immunology, Division of Comparative Medicine, Division of Animal Care, Vanderbilt University Medical Center, Nashville, Tennessee; [2]Department of Veterinary Biosciences, The Ohio State University, Columbus, Ohio; [3]Department of Biostatistics, Vanderbilt University Medical Center, Nashville, Tennessee

**Corresponding authors. Emails: rachel.howie@vumc.org or katherine.gibson-corley@vumc.org*

of blood after death), putrefaction (bacterial proliferation), gastrointestinal (GI) distension (gas formation from anaerobic bacteria), destruction of muscle fiber integrity, and fluid from orifices can be visualized.[1,5,16] Changes such as autolysis, loss of overall cellular architecture, cell membrane degradation, and saprophytic bacteria must be identified histologically.[5,10]

We hypothesized that specific histopathologic changes associated with postmortem changes would occur in a time and temperature-dependent manner in mouse tissues. We further hypothesize that refrigerated storage will slow autolysis in mouse carcasses by 3 d as compared with storage at RT. Our goal in this study was to evaluate the PMI of mice at RT and under refrigeration to determine a threshold for the diagnostic utility of necropsy. For this study, we designed a comprehensive system for the analysis of autolysis and semiquantifiable histomorphologic criteria of autolysis for use in mice.

Materials and Methods

Animal housing and husbandry. One hundred and eight adult, male and female, experimentally naïve C57BL/6 mice born at our institution were used in this study. All mice were nulliparous and 8 to 12 mo of age. In keeping with the *Three R's Guidelines* (replacement, refinement, and reduction) from the *Guide for the Care and Use of Laboratory Animals* in terms of reduction, mice were selected from cages designated for euthanasia by investigators. Mice were selected from colonies that were free of microbial pathogens, endoparasites (pinworms *Syphacia* spp. and *Aspiculuris* spp.), ectoparasites (fur mites *Myobia musculi*, *Mycoptes musculinis*, *Radfordia affinis*, and *Psorergates* simplex) and viruses (mouse hepatitis virus, mouse parvovirus, minute virus of mice, lymphocytic choriomeningitis virus, Sendai virus, pneumonia virus of mice, mouse rotavirus, Theiler mouse encephalomyelitis virus, ectromelia virus, mouse adenovirus, mouse reovirus) based on a dirty bedding sentinel program and direct screening of incoming mice. Before euthanasia, mice were housed in autoclaved polysulfone IVC on irradiated cellulose paper bedding (Alpha-Dri; Shepherd Specialty Papers), fed standardized rodent chow (5010 diet; Purina Mills International, St. Louis, MO), and given hyperchlorinated water ad libitum by water bottle. The IVC rack was set to 60 air changes per hour. Housing room conditions included a 12:12-h light:dark cycle, a temperature of 68 to 72 °F (20 to 22 °C), relative humidity of 30% to 70%, and room ventilation of 10 to 15 air changes per hour. All animal manipulations were approved by the Institutional Animal Care and Use Committee of Vanderbilt University Medical Center, an AAALAC-accredited institution.

Experimental design. Mice were euthanized in their home cage using carbon dioxide at a flow rate of 30% to 70% volume displacement per minute (Euthanex Smart Box Auto CO2 System, model V700). Cervical dislocation was performed as a secondary method of euthanasia. Each mouse was then weighed. After euthanasia, mice were randomized into groups of 3 without regard to sex and randomly assigned an individual time point for postmortem evaluation. Fifty-four mice each were allocated to the refrigeration (4 °C) and the RT (20 to 22 °C) cohorts. Three mice from each cohort were evaluated immediately after euthanasia (time 0) and at hours 4, 8, and 12 and days 1, 2, 3, 4, 5, 6, 7, 8, 9, 10, 11, 12, 13, and 14 after euthanasia, resulting in a total of 18 time points, including 0 (Figure 1). Carcasses from the refrigeration cohort were placed in ventral recumbency in a biohazard bag and stored at 4 °C until PMI evaluation; RT carcasses were placed in ventral recumbency in an autoclaved polysulfone microisolation cage (11.75 × 7.25 × 5 in.; Allentown Caging, Allentown, NJ) on a negatively ventilated rack (Allentown 12 ATU) with an air change rate of 60 changes per hour (Figure 2A and B). To mimic the normal mouse microenvironment, 25 mL of soiled bedding from the home cage was added to 400 mL of clean bedding in the new cage.[23] The room was maintained on a 12:12-h light:dark cycle and humidity of 40% to 70%. Carcass temperatures and intracage ammonia levels were measured daily. In both treatment groups, PMI evaluation included assessment of weight, gross pathology, necropsy with histologic assessment, and internal and external photographs.

PMI gross evaluation and scoring. Gross body scores were assigned at all time points based on the presence or absence of predefined characteristics. Characteristics evaluated were skin tenting (how easily the skin stays in position after being pinched), skin fragility (how easily skin could be torn by hand), rigor mortis (stiffening of the joints and muscles), GI distension (expansion of the intestinal loops with gas/fluid), livor mortis (gravity dependent pooling of blood), organ adherence (autolyzed organs that could not be retracted from the body wall), bile imbibition (green discoloration from bile leakage), and peripheral tissue desiccation (extreme skin dryness characterized by necrotic and sloughing skin or the drying out of mucous membranes). Before full necropsy, which included examination, dissection, and collection of all listed tissue samples into 12 individual cassettes, a gross photograph was taken in

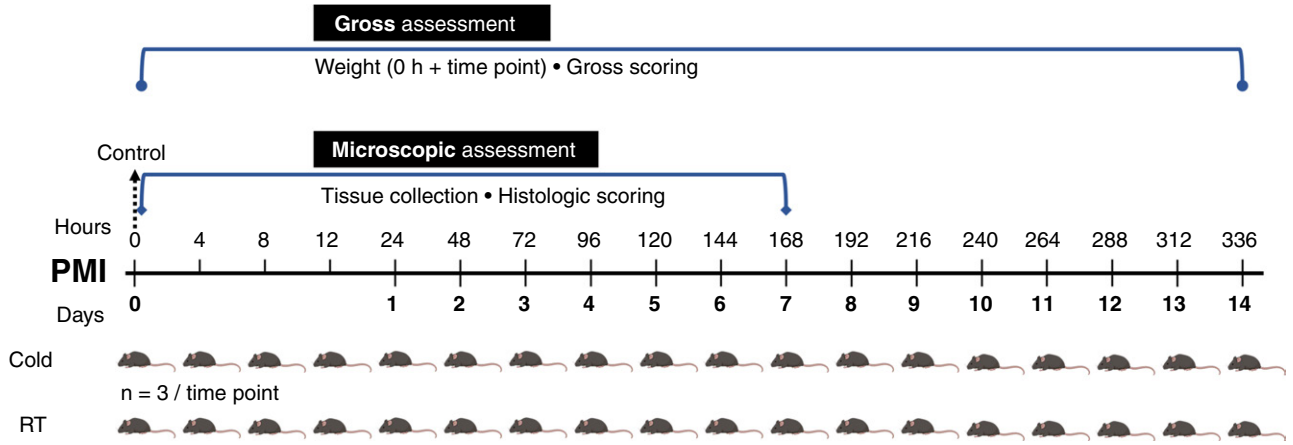

Figure 1. Experimental design and postmortem interval timeline, including procedures across all treatment groups. Note that one schematic mouse represents an *n* = 3 at each time point.

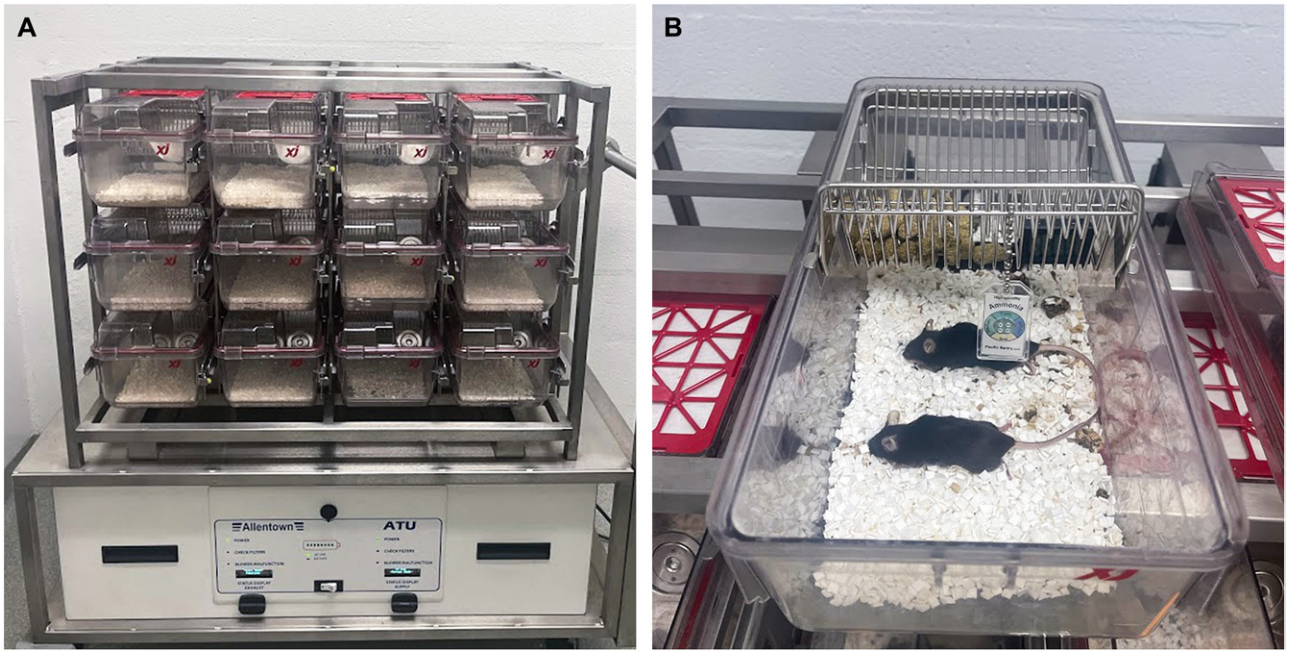

Figure 2. Representative schematic image of the room temperature cohort's rack (A) and carcass cage layout (B) before a full tissue collection.

ventral and dorsal recumbency. In addition, a ventral incision was made, from pubis to mandible and an internal gross photograph was taken.

PMI histopathologic evaluation and scoring. Necropsy and tissue collection were performed at the indicated time points up to 14 d. Tissues collected included the brain within the skull, heart, lung, liver, kidney, spleen, pancreas, quadriceps skeletal muscle, and gastrointestinal tract (stomach, small intestines, cecum, and colon). The lungs and cecum were insufflated with 2 mL of neutral buffered formalin (lot no. 129078, cat. no. C4320-105) prior to immersion for fixation. All tissues were fixed in at least 50 mL of formalin (10% buffered; lot. no. 129078, cat. no. C4320-105; CardinalHealth) for 48 h at RT. Decalcification of the head was performed with 20 mL of formic acid solution (Immunocal; lot no. 162933, cat. no. 1414-2; StatLab) for an additional 48 h at RT after fixing. All tissues from all mice were trimmed, processed, embedded in paraffin, sectioned at 5 µm, and stained with hematoxylin and eosin. Tissues were then examined histologically and scored for rates of autolysis by an individual who was blind to the treatment group and was overseen by a board-certified veterinary pathologist.

Autolysis was evaluated using a semiquantitative scale, with different severity criteria for each tissue (see Results section). Key cellular features of autolysis such as loss of cellular detail, cytoplasmic eosinophilia, karyolysis, peripheralized organ pallor, etc., were noted on an ordinal scale. To maximize detection and repeatability, an ordinal scale of 0 to 3 was used to indicate, as compared with time 0, no change (0%), mild change (< 25%), moderate change (25% to 75%), and severe change (> 75%), with more detailed characteristics provided in Table 1.[14] The overall histology score for each mouse was obtained by summing the individual component scores.

Image acquisition. Photomicrographs were taken using an Olympus BCX53 microscope and an Olympus UC90 camera using Olympus CellSens software.

Daily cage-side evaluation. In the RT aim of the study, carcass temperature, ammonia levels, humidity levels, and cage temperature were measured daily. The room was checked twice daily for temperature and humidity. Carcass temperature was measured using an infrared thermometer gun (Benetech; ASIN: B08Q3K43BC). Humidity and temperature were measured using a Thermohygrometer (TAIWEI001; ASIN: B07MCGDN5C; model no. 8541833479). Ammonia levels were measured using ammonia sensors (Pacific Sentry) and colorimetric ammonia strips (Hydrion; lot no. 210321). In the refrigerated group, temperature was monitored and remained at 4 °C for the entire study.

Statistical analysis. We used a sample size of 3 mice per time point per treatment group due to the descriptive nature of this study. Each mouse was treated as a single unit of analysis in each group per time point. The baseline weights of RT and refrigerated carcasses were assessed using a *t* test with unequal variance. For each PMI attribute, we observed the number of carcasses exhibiting this attribute at each time point in mice kept at room and refrigerated temperatures. The distribution of these numbers of mice from the RT and refrigerated-temperature groups was compared using 2-sample Kolmogorov-Smirnov tests. The percent change in weight from baseline (percent change) was assessed by a linear regression model with a zero *y*-intercept (at baseline the percent change was zero). This model regressed percent change against time after death and a treatment-time interaction covariate. The analysis of the change in histology score with time and treatment used a multivariable regression model. This change was linear in the refrigerated cohort but nonlinear in the RT cohort. The best fit for histology scores in RT carcasses was obtained with a 6-kn cubic spline model.[15] The Akaike information criterion was used to select the optimal number of knots.

Results

The average baseline (time 0) weights in the newly euthanized and predetermined refrigerated and RT cohorts were significantly different from each other (27.6 g [SD = 2.5] and 25.4 g [SD = 4.6], respectively; $P = 0.003$). The weight of the RT carcasses fell significantly more over time as compared with those in the refrigerated group (Figure 3). The total percentage of weight loss over the course of the study was approximately 16% for the RT cohort and 1% for the refrigerated cohort. Mice at RT

Table 1. Tissue-specific scores used by reviewers who were blind to the group to provide qualitative assessment of autolysis

Tissue	Value	Criteria
Lung	0	No apparent changes
	1	Peripheralized pallor of tissue
	2	Peripheral pallor, hypereosinophilia of cells, minimal sloughing of airway epithelium
	3	Peripheral pallor, hypereosinophilia of cells, moderate to severe sloughing of airway epithelium
Stomach/GI	0	No apparent changes
	1	<25% sloughing of gastric mucosa + loss of villous/glandular architecture
	2	25%–75% sloughing of gastric mucosa + loss of villous/glandular architecture
	3	>75% sloughing of gastric mucosa + loss of villous/glandular architecture
Pancreas	0	No apparent changes
	1	<25% loss of exocrine cell detail, loss of zymogen granules, loss of tissue architecture
	2	25%–75% loss of exocrine detail, loss of zygomen granules, loss of tissue architecture
	3	>75% loss of exocrine detail, loss of zygomen granules, loss of tissue architecture
Spleen	0	No apparent changes
	1	<25% cell dissociation + peripheralized pallor, loss of cellular detail
	2	25%–75% cell dissociation + peripheralized pallor loss of cellular detail
	3	>75% cell dissociation + peripheralized pallor, loss of cellular detail
CNS	0	No apparent changes
	1	<25% neuronal vacuolation and/or loosening of neuropil
	2	25%–75% neuronal vacuolation and/or loosening of neuropil
	3	>75% neuronal vacuolation and/or loosening of neuropil
Liver	0	No apparent changes
	1	Cell dissociation
	2	Cell dissociation + pericapsular pallor
	3	Cell dissociation + pericapsular pallor + loss of hepatocellular cytoplasmic detail
Kidney	0	No apparent changes
	1	<25% tubule epithelial sloughing, hypereosinophilia, and loss of cellular detail
	2	25%–75% tubule epithelial sloughing, hypereosinophilia, and loss of cellular detail
	3	>75% tubule epithelial sloughing, hypereosinophilia, and loss of cellular detail
Heart	0	No apparent changes
	1	<25% loss of cross striations + pyknosis
	2	25%–75% loss of cross striations + pyknosis
	3	>75% loss of cross striations + pyknosis
Smooth muscle	0	No apparent changes
	1	<25% loss of cross striations + pyknosis
	2	25%–75% loss of cross striations + pyknosis
	3	>75% loss of cross striations + pyknosis

GI, gastrointestinal.

lost 0.78% of their baseline body weight per day as compared with 0.06% for refrigerated mice (95% CI for difference of 0.67% to 0.76%, $P < 0.0005$).

Gross findings. Gross changes were assessed and scored before and during necropsy on all mice at all time points (Table 2). Gross parameters assessed for each mouse were time of onset and resolution of rigor mortis, skin tenting, skin fragility, GI distention, livor mortis, peripheral tissue desiccation, organ adherence, and bile imbibition. Concordant findings of present or absent were found in the 2 experimental groups at each time point for the following features: time of onset and resolution of rigor mortis, skin tenting, skin fragility, and bile imbibition (Table 2). Both experimental groups showed an onset of rigor mortis at 4 h after euthanasia, and rigor mortis was no longer present on day 3. Both experimental groups showed skin tenting beginning at 4 h postmortem and present thereafter at all remaining time points. Skin fragility was observed in both groups on day 6 in the refrigerated cohort and day 7 in the RT cohort and persisted in both groups throughout all later time points. Bile imbibition was present at 12 h in the refrigerated cohort and 8 h in the RT cohort.

In contrast, the 2 experimental groups showed different patterns of GI distention, livor mortis, peripheral tissue desiccation, and organ adherence (Table 2). GI distension was not observed in the refrigerated cohort but appeared in the RT cohort at 4 d and remained until 13 d postmortem ($P < 0.0005$). Livor mortis appeared at 7 d in the refrigerated cohort and at 8 h in the RT cohort and in both groups lasted throughout all later time points ($P < 0.0005$). Peripheral tissue desiccation was observed on day 10 in the refrigerated cohort and day 9 in the RT cohort. Organ adherence occurred in the refrigerated and RTs cohorts on days 10 and 7, respectively. Representative photographs of these changes are shown in Figure 4.

Histologic findings. Evaluation of autolysis was based on a scoring system to provide a semiquantitative value, which was specific to each tissue collected (Table 1). Visual autolysis

per select tissue per time point can be seen in Figure 5. Representative images of the lung, spleen, small intestine, liver, and kidney at time points zero (control), 1, 4, and 7 d PMI are represented. In lung tissue, sloughing of airway epithelium and peripheralized organ pallor were observed at 1 d in the RT cohort, while in the refrigerated cohort was not observed until day 4. In the spleen, loss of cellular detail and architecture was observed within 12 h at RT cohort but not until day 6 when refrigerated. In the small intestine of the RT cohort, sloughing of enterocytes and loss of villous architecture were observed at 4 h, and in the refrigerated cohort, similar changes were observed at day 1. In the liver, there was intercellular dissociation and loss of hepatocellular detail at 8 h, and in the refrigerated cohort, this was observed on day 4. Finally, in the kidney, tubular epithelial sloughing and loss of cellular detail were observed at 8 h, and in the refrigerated cohort, this was observed at day 2. Other tissues assessed per animal were the pancreas, CNS, heart, and smooth muscle. In the pancreas, at RT, loss of cellular detail, including zymogen granule loss and pancreatic architecture disruption was observed at 4 h, while in the refrigerator this did not become observed until day 1. In the CNS, at RT, rarefaction of the neuropil and neuronal vacuolation was observed at 1 d, while in the refrigerated cohort, this was not observed until day 4. Finally, in the heart at RT, loss of cross striations and nuclear detail in cardiac myocytes was observed at 1 d, while in the refrigerated cohort, this was not observed until day 4. In smooth muscle at RT, similar changes to those in the heart were observed at 12 h, while in the refrigerated cohort, this was not observed until day 3.

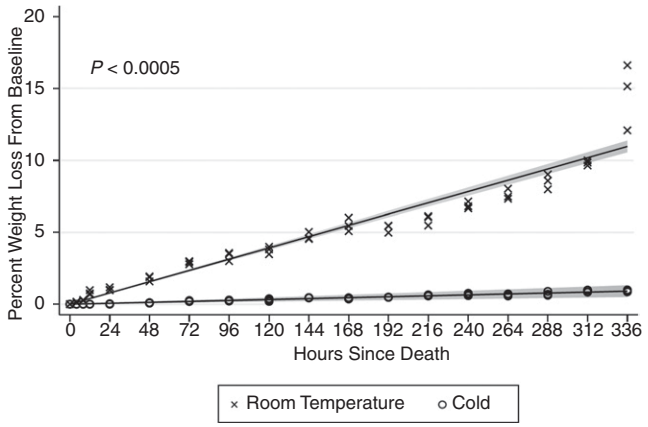

Figure 3. Weight percentage decrease over time was significant between carcasses that were stored in the refrigerator (o) and those at room temperature (x). Each mouse was individually scored as a single unit of measurement and statistically analyzed. The representative gray shading indicates a 95% confidence interval and $P < 0.0005$.

In every mouse, after a necropsy was performed, each tissue was individually scored (Table 3) based on variable autolytic criteria, and the total cumulative score per group per time point was assessed (Figure 6). With a 95% confidence interval (as seen in the gray-shaded area for both experimental groups), there was a significant increase in autolysis in both treatment groups ($P < 0.0005$). However, the rate of increase was markedly greater in the RT cohort during the first 24 h after death ($P < 0.00005$). Thereafter, the rate of increase in both treatment groups was approximately equal. As compared with the refrigerated cohort over time, the effects of both time and treatment were highly significant between both cohorts. Moreover, the interaction is also significant, with the rate of increase of total score with time in the RT cohort being significantly greater than in the refrigerated cohort.

Macroenvironmental parameters. Humidity, temperature, and ammonia levels were measured daily for the RT cohort. In all cages, ammonia levels were between 0 to 5 ppm and did not differ significantly across PMI time points. The average humidity was 53%. The average temperature was 21 °C.

Discussion

A paucity of information in the literature underlies a significant knowledge gap with regard to the accuracy and precision of methods used to determine PMI, and no single method of estimation is widely accepted to date.[5,10] Due to the diversity of species and environmental factors, human methods such as body temperature-based systems are unreliable.[5] That method, also known as the Hennsige Nomogram method, calculates the rate of body cooling to estimate PMI. Other factors used to determine PMI in humans are based on entomology and the potassium concentration of the vitreous humor.[18,25] These methods are not useful for individual animals in a well-controlled research environment.[17] Furthermore, human methods are subject to extrinsic factors such as clothing, insulation, and intrinsic factors such as illness, injury, and resuscitation attempts.[1,6]

The accurate estimation of PMI and an understanding of postmortem changes are important with regard to diagnostics, health surveillance, forensics, and harvesting of game.

Table 2. System used to score gross postmortem changes

	Time point																	
Gross change	0 h	4 h	8 h	12 h	24 h	2 d	3 d	4 d	5 d	6 d	7 d	8 d	9 d	10 d	11 d	12 d	13 d	14 d
Rigor mortis		•	•	•	•	•	•											
Skin tenting		•	•	•	•	•	•	•	•	•	•	•	•	•	•	□	□	□
Skin fragility										□	•	•	•	•	•	•	•	•
GI distention								Δ	Δ	Δ	Δ	Δ	Δ	Δ	Δ	Δ	Δ	
Livor mortis		Δ	Δ	Δ	Δ	Δ	Δ	Δ	Δ	Δ	•	•	•	•	•	•	•	•
Tissue desiccation											Δ	Δ	Δ	•	•	•	•	•
Organ adherence											Δ	Δ	Δ	•	•	•	•	•
Bile imbibition				•	•	•	•	•	Δ	Δ	Δ	•	•	•	•	•	•	•

Dots indicate that the indicated postmortem change was present in both groups at the indicated time point indicated in both groups; squares indicate that the change was found only in the refrigerated cohort; and triangles indicate that the change was found only in the room temperature cohort at the indicated time points.

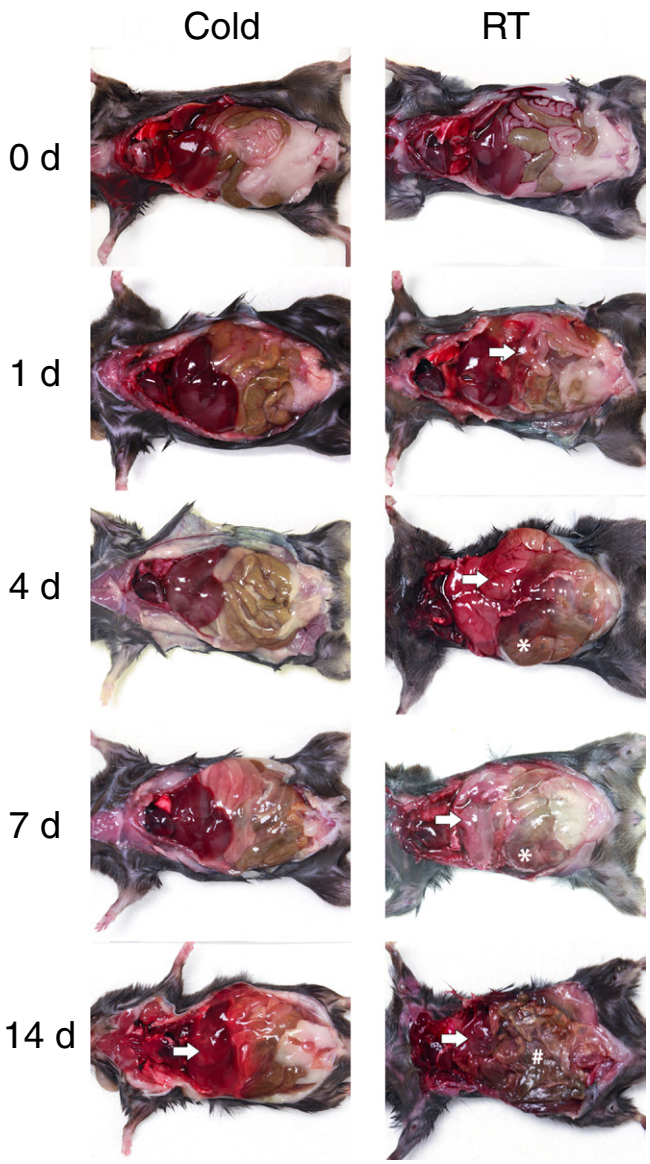

Figure 4. Representative gross decomposition images of the thoracic and abdominal cavities at key time points postmortem in the cold cohort (left) and room temperature cohort (RT) (right) at 0, 1, 4, 7, and 14 d. Asterisks: intestinal distension; arrows: livor mortis; hash mark: tissue desiccation).

Postmortem changes occur as a continuum after death and can be termed decompositional changes. Decompositional changes include 2 parallel processes: autolysis and putrefaction.[11] These changes are classified as immediate, early, and late.[1] They involve complex biologic and cellular modifications that are affected by intrinsic and extrinsic factors. Understanding the appearance, progression, and timings of postmortem changes is essential in estimating PMI for each tissue.[1] Various tissues have different rates of autolysis that are influenced by the environment. Autolysis depends on both environmental temperature, tissue-specific enzymatic processes, disease, age, and species.[13] Because postmortem changes and the rates of change in various tissues are influenced by many factors, including ambient temperature, PMI cannot be accurately estimated based on any single postmortem change.[1,6]

To date, postmortem changes have not been compared with regard to animal carcasses stored in a refrigerated environment or found after remaining at ambient temperatures for unknown periods of time in the home cage. Our study shows that refrigeration significantly slows postmortem changes in general as compared with RT and at different time points for different tissues. Our results indicate that if necropsy and fixation cannot be performed immediately after death, refrigeration of carcasses can maintain gross tissue quality for 7 d as compared with 2 d at RT. Our study has provided a general scale for the evaluation of postmortem tissue changes in mice and offers guidance on how long tissues from carcasses remain adequate for postmortem interpretation. As is available for humans,[5,9,25] future studies in this area could provide a database with information on how long after death specific animal tissues can be validly assessed and interpreted.

With regard to weight, our RT cohort lost significantly more weight than the refrigerated group. The average percent weight loss per hour was 1% at RT and 0.1% under refrigeration. The significant weight loss at RT is likely due to desiccation, autolysis, and tissue breakdown.[4,5] As cells die, ion gradients are no longer maintained, leading to loss of cell membrane integrity.[4] The cell then becomes exposed to proteolytic enzymes that further degrade the cell, resulting in decay and loss of total body weight.[4,5] Grossly, immediately after death the body begins to undergo putrefaction that leads to desiccation.[5] Various external factors have complementary effects, some having an early postmortem time of onset and then resolving with time; some gross postmortem changes accumulate but others resolve.[13] As seen in our study, under both experimental temperatures, the general pathway of gross changes carcasses involved muscle rigidity defined by rigor, tenting of the skin (indicative of dehydration or overall desiccation of the skin), livor mortis (the pooling of blood due to gravity), bile imbibition (which appears as green discoloration of hemoglobin being denatured to biliverdin in a putrefaction process), and skin fragility (indicative of generalized decay).[4,17] Other noncomplementary changes are organ adherence to the skin (indicative of liquefaction and severe autolysis), peripheral tissue desiccation (the drying out of mucous membranes dependent on temperature), and GI distention (the process of gas formation from anaerobic bacteria through decay).[5]

Histologic damage from autolysis appears as microstructural changes that occur in most tissues and show loss of cellular stain uptake, tissue architecture, and cellular detail.[9] Autolytic changes should not be misinterpreted as tissues undergoing necrosis, which is unprogrammed and irreversible cell death due to exogenous cellular injury.[9,12,27,29] To accurately assess PMI with autolytic interference, specific criteria were needed to allow proper interpretation of PMI in individual tissues. In our study, the greatest histologic change occurred in the small intestine, spleen, liver, kidney, and pancreas. The least histologic change occurred in the lung, heart, CNS, and smooth muscle. In general, autolysis causes liquefaction of tissues by releasing phosphorus-rich intracellular enzymes, most often lytic enzymes that include alkaline and acid phosphatases, ATP, 5′-nucleotidases, and glucose-6-phosphatase from lysosomes.[9,13,29] These autolytic processes are tissue specific, and autolysis will occur more rapidly in some tissues due to higher enzyme content. For example, we did not assess the gallbladder because it undergoes rapid autolysis due to the cytolytic action of bile acids.[1,2,7]

Autolysis can also be accelerated by red blood cell degradation and hemolysis, and some cells are especially sensitive to hypoxia, leading to ischemia and cessation of metabolic activity.[8,13,21,29] Erythrocytes degrade faster depending on their tissue location.[8] For example, in the liver, red blood cells

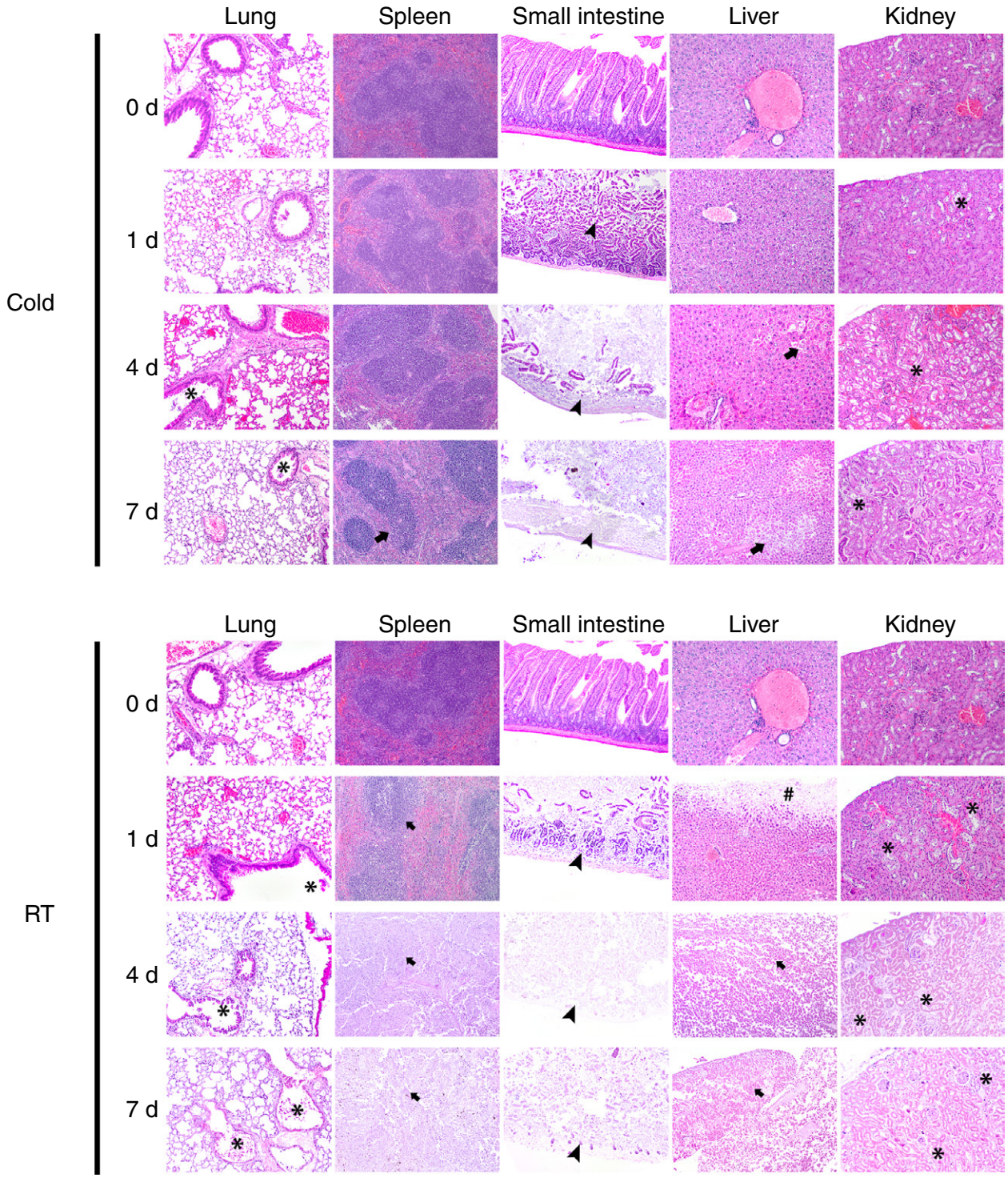

Figure 5. Representative photomicrographs of the H and E-stained tissues from the lung, spleen, small intestine, liver, and kidney over time in refrigeration (top) and room temperature (bottom). Slides were scored based on the scoring system for autolysis. Asterisks: epithelial sloughing; arrows: intercellular dissociation and loss of tissue architecture; arrowheads: intestinal villus epithelial sloughing and loss; hash mark: pericapsular pallor. All images were taken at 20× magnification.

degrade faster in the sinusoidal space than they do in the lung parenchyma.[8,22,24] Intestinal mucosa and pancreatic parenchyma autolyze more rapidly than neuronal and connective tissue because the latter contain hypoxia-resistant cells.[20,29] Given that most tissue activity is oxygen dependent, autolysis and gross decay are slowed at refrigeration temperatures. However, even though refrigeration slows degradation, freezing carcasses before postmortem evaluation is not recommended. Freezing tissues is sometimes useful, but for diagnostic and especially histologic evaluation, freezing will produce tissue artifacts such as ice crystal formation and require thawing.[26]

Daily cage humidity, temperature, and ammonia levels did not change significantly over the course of the study for the RT cohort and were within acceptable target parameters throughout the course of the study according to the *Guide for the Care and Use of Laboratory Animals Recommendations*.[21] All ammonia sensors

Table 3. Cumulative histopathology scores of mice in each group (n = 3 per group) and total score per group

Group	Time	Lung	GIT	Pancreas	Spleen	Brain	Liver	Kidney	Heart	Muscle	Total
Cold	0 h	—	—	—	—	—	—	—	—	—	0
Cold	4 h	—	1	—	—	—	—	—	—	—	1
Cold	8 h	—	1	1	—	—	—	—	—	—	2
Cold	12 h	—	1	1	—	—	—	—	—	—	2
Cold	24 h (1 d)	—	3	3	—	—	—	2	—	—	8
Cold	2 d	—	4	3	—	—	2	3	3	—	15
Cold	3 d	—	5	4	—	2	3	5	3	1	23
Cold	4 d	2	6	5	1	4	4	5	3	2	31
Cold	5 d	2	6	5	3	3	5	6	4	3	37
Cold	6 d	3	6	6	4	4	6	6	4	3	42
Cold	7 d	3	6	6	5	5	6	6	6	5	48
RT	0	—	—	—	—	—	—	—	—	—	0
RT	4 h	—	3	3	—	—	—	3	1	—	10
RT	8 h	—	5	3	1	—	3	3	1	1	17
RT	12 h	2	6	3	2	1	3	3	3	2	25
RT	24 h (1 d)	3	8	5	3	3	5	5	3	3	38
RT	2 d	3	9	8	6	3	6	7	3	3	48
RT	3 d	4	9	9	8	4	7	8	4	3	56
RT	4 d	6	9	9	9	6	9	9	4	3	64
RT	5 d	8	9	9	9	6	9	9	6	6	71
RT	6 d	9	9	9	9	8	9	9	6	6	74
RT	7 d	9	9	9	9	9	9	9	7	6	76

Cold, refrigerated carcasses; GIT, gastrointestinal; RT, room temperature carcasses.

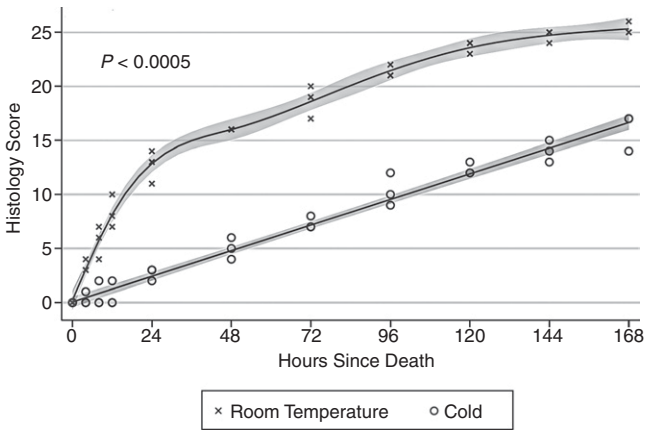

Figure 6. Quantification of the histologic scoring system for postmortem interval assessing autolysis over time at room temperature (x) and refrigeration (o). Each mouse was individually scored as a single unit of measurement and statistically analyzed. The representative gray shading indicates a 95% confidence interval with a 6-kn restricted cubic spline covariance.

detected ammonia at levels of "low readings," indicating levels between 0 and 1 ppm. This level was confirmed by the ammonia strips placed on the bottom of the cages, which recorded levels of 0 to 5 ppm. Humidity ranged from 50% to 55% inside the cage and in the room. The temperature in the room and cage stayed between 20 and 22 °C. These levels are similar to humidity and temperature parameters that would occur in a typical populated cage.[3,22] Refrigeration temperatures and humidity remained at 4 °C and 35% to 40%, respectively, throughout the study.

Although we measured postmortem change on a daily basis, future studies could use a larger number of mice, time points, and tissues could more accurately determine the rate of PMI. A more precise PMI database and scale should test variations such as refrigeration after delayed discovery, intracage ammonia concentrations, husbandry practices such as bedding, cage types, microenvironmental parameters such as temperature and humidity, presence of cage mates, and different strains of mice, including germfree. This would allow the individuals who find mouse carcasses to immediately assess suitability for necropsy. Research animal medicine already uses a weaning scale, a grimace scale, and a coat color by strain scale; but to date does not have a visual scale for assessing postmortem changes.[19] A scale with known gross and histologic changes would reduce the number of unnecessary necropsies and thus allow veterinarians and researchers to save time, money, and labor. Additional studies would also be needed for the formulation of a standardized gross and histologic scoring system for specific tissues to further refine the PMI.

Limitations to our study include our use of only one mouse strain and one single type of cage, rack, and bedding. Evaluation of germ-free or immunodeficient mice and their microbiomes would expand our knowledge with regard to gastrointestinal dissimilarities. Another limitation was that we placed only three mice in each cage; therefore, we could not evaluate potential fluctuations in humidity, ammonia, and temperature levels that may result from a higher cage population, perhaps including live mice.[3] Also, the average weight of the refrigerated cohort at baseline was 2.17 g heavier than that of the RT mice. However, we believe that this difference would not affect our findings. An additional limitation to our study is only assessing PMI up to 14 d. Extending the evaluation period to 21 d to mimic a 21-d cage change interval would provide a larger database of PMI.

In conclusion, our study evaluated and refined the estimation of PMI in mice. Our data show that as compared with RT, refrigeration of carcasses significantly slows decomposition. Furthermore, the PMI suitable for performing informative necropsies is 5 d with refrigeration and 1 d at RT. Based on our findings, we have provided information to inform

diagnosticians about the viability of different tissues of interest for a range of PMIs. It is recommended that institutions either perform necropsies on recently deceased mice or immediately place the carcass in the refrigerator for preservation.

Acknowledgments

We thank the staff in the Translational Pathology Shared Resource for their guidance and expertise.

Conflict of Interest

The authors have no conflicts of interest to declare.

Funding

The Translational Pathology Shared Resource is supported by NCI/NIH Cancer Center Support Grant P30CA068485. This work was internally funded by Vanderbilt University Medical Center.

References

1. **Almulhim AM, Menezes RG.** [Internet]. 2023. Evaluation of postmortem changes. In: StatPearls. Treasure Island (FL): StatPearls Publishing. [Cited 1 May 2023]. Available at: https://www.ncbi.nlm.nih.gov/books/NBK554464
2. **Azarpira N, Rastegar F, Amiri M, Esfandiari E, Geramizadeh B.** 2012. Comparison of cytotoxic activity of bile on HepG2 and CCRF-CEM cell lines: An in vitro study. Iran J Med Sci **37**:266–270.
3. **Bailoo JD, Murphy E, Varholick JA, Novak J, Palme R, Würbel H.** 2018. Evaluation of the effects of space allowance on measures of animal welfare in laboratory mice. Sci Rep **8**:713. https://doi.org/10.1038/s41598-017-18493-6
4. **Boyd EM, Knight LM.** 1963. Postmortem shifts in the weight and water levels of body organs. Toxicol Appl Pharmacol **5**:119–128. https://doi.org/10.1016/0041-008X(63)90086-3
5. **Brooks JW.** 2016. Postmortem changes in animal carcasses and estimation of the postmortem interval. Vet Pathol **53**:929–940. https://doi.org/10.1177/0300985816629720
6. **Ceciliason AS, Andersson MG, Lindström A, Sandler H.** 2018. Quantifying human decomposition in an indoor setting and implications for postmortem interval estimation. Forensic Sci Int **283**:180–189. https://doi.org/10.1016/j.forsciint.2017.12.026
7. **Ceciliason AS, Andersson MG, Nyberg S, Sandler H.** 2021. Histological quantification of decomposed human livers: A potential aid for estimation of the post-mortem interval. Int J Legal Med **135**:253–267. https://doi.org/10.1007/s00414-020-02467-x
8. **Celata EN.** 2015. Postmortem intervals in mice submerged in aqueous environments at 20°C. J Forensic Sci **60**:1495–1499. https://doi.org/10.1111/1556-4029.12850
9. **Cocariu EA, Mageriu V, Stăniceanu F, Bastian A, Socoliuc C, Zurac S.** 2016. Correlations between the autolytic changes and postmortem interval in refrigerated cadavers. Rom J Intern Med **54**:105–112. https://doi.org/10.1515/rjim-2016-0012
10. **Erlandsson M, Munro R.** 2007. Estimation of the post-mortem interval in beagle dogs. Sci Justice **47**:150–154. https://doi.org/10.1016/j.scijus.2007.09.005
11. **French K, Jacques R.** [Internet]. Postmortem changes. PathologyOutlines.com website. [Cited 16 January 2024]. Available at: https://www.pathologyoutlines.com/topic/forensicspostmortem.html
12. **Galluzzi L, Vitale I, Aaronson SA, Abrams JM, Adam D, Agostinis P, Alnemri ES.** 2018. Molecular mechanisms of cell death: Recommendations of the nomenclature committee on cell death. Cell Death Differ **25**:486–541. https://doi.org/10.1038/s41418-017-0012-4
13. **George J, van Wettere AJ, Michaels BB, Crain D, Lewbart GA.** 2016. Histopathologic evaluation of postmortem autolytic changes in bluegill (*Lepomis macrohirus*) and crappie (*Pomoxis anularis*) at varied time intervals and storage temperatures. PeerJ **4**:e1943. https://doi.org/10.7717/peerj.1943
14. **Gibson-Corley KN, Olivier AK, Meyerholz DK.** 2013. Principles for valid histopathologic scoring in research. Vet Pathol **50**:1007–1015. https://doi.org/10.1177/0300985813485099
15. **Harrell FE.** 2015. Regression modeling strategies: With applications to linear models, logistic regression, and survival analysis, 2nd ed. New York (NY): Springer.
16. **Henssge C, Wang H, Hoppe B.** 2002. Light microscopical investigations on structural changes of skeletal muscle as artifacts after postmortem stimulation. Forensic Sci Int **125**:163–171. https://doi.org/10.1016/S0379-0738(01)00634-X
17. **Matuszewski S.** 2021. Post-mortem interval estimation based on insect evidence: Current challenges. insects **12**:314. https://doi.org/10.3390/insects12040314
18. **Metcalf JL, Wegener Parfrey L, Gonzalez A, Lauber CL, Knights D, Ackermann G, Humphrey GC, et al.** 2013. A microbial clock provides an accurate estimate of the postmortem interval in a mouse model system. eLife **2**:e01104. https://doi.org/10.7554/eLife.01104
19. **MouseMine, Mouse Genome Informatics Web Site.** [Internet]. Bar Harbor (ME): The Jackson Laboratory. [Cited 1 October 2023]. Available at: http://www.mousemine.org/
20. **Ogata J, Yutani C, Imakita M, Ueda H, Waki R, Ogawa M, Yamaguchi T, Sawada T, Kikuchi H.** 1986. Autolysis of the granular layer of the cerebellar cortex in brain death. Acta Neuropathol **70**:75–78. https://doi.org/10.1007/BF00689517
21. **Palić M, Džaja P, Gudan Kurilj A, Severin K, Šerić Jelaska L.** 2021. Assessment of post-mortem interval based on post-mortem changes and entomological findings. Vet Stn **52**:113–123.
22. **Peters A, Festing M.** 1990. Population density and growth rates in laboratory mice. Lab Anim **24**:273–279. https://doi.org/10.1258/002367790780866227
23. **Smith PC, Nucifora M, Reuter JD, Compton SR.** 2007. Reliability of soiled bedding transfer for detection of mouse parvovirus and mouse hepatitis virus. Comp Med **57**:90–96.
24. **Splitter GA, McGavin MD.** 1974. Sequence and rate of postmortem autolysis in guinea pig liver. Am J Vet Res **35**:1591–1596.
25. **Sturner WQ, Gantner GE Jr.** 1964. The postmortem interval. A study of potassium in the vitreous humor. Am J Clin Pathol **42**:137–144. https://doi.org/10.1093/ajcp/42.2.137
26. **Taqi SA, Sami SA, Sami LB, Zaki SA.** 2018. A review of artifacts in histopathology. J Oral Maxillofac Pathol **22**:279. https://doi.org/10.4103/jomfp.JOMFP_125_15
27. **Trump BF, Berezesky IK, Chang SH, Phelps PC.** 1997. The pathways of cell death: Oncosis, apoptosis, and necrosis. Toxicol Pathol **25**:82–88. https://doi.org/10.1177/019262339702500116
28. **Vesell ES, Lang CM, White WJ, Passananti GT, Hill RN, Clemen TL, Liu DL, Johnson WD.** 1979. Environmental and genetic factors affecting response of laboratory animals to drugs. Fed Proc **35**:1125–1132.
29. **Wenzlow N, Neal D, Stern AW, Prakoso D, Liu JJ, Delcambre GH, Beachboard S, Long MT.** 2021. Feasibility of using tissue autolysis to estimate the postmortem interval in horses. J Vet Diagn Invest **33**:825–833. https://doi.org/10.1177/10406387211021865